Constant-Charge Reaction Theory for Potential-Dependent Reaction Kinetics at the Solid−Liquid Interface
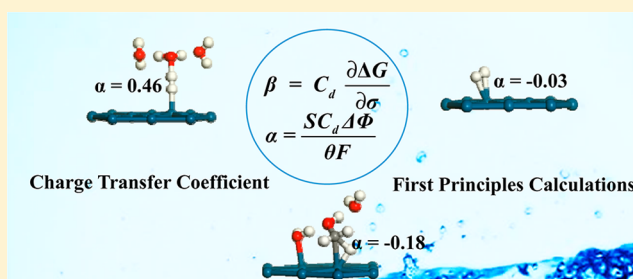
Ya-Hui Fang,[†,‡] Guang-Feng Wei,[‡] and Zhi-Pan Liu*,[‡]

[†]School of Chemical and Environmental Engineering, Shanghai Institute of Technology, Shanghai 201418, China
[‡]Shanghai Key Laboratory of Molecular Catalysis and Innovative Materials, Department of Chemistry, Key Laboratory of Computational Physical Science (Ministry of Education), Fudan University, Shanghai 200433, China

S *Supporting Information*

ABSTRACT: To understand the potential-dependent kinetics of reactions at the solid−liquid interface, we derive a constant-charge reaction theory for understanding the coupled charge transfer during the chemical bond making/breaking. The charge transfer coefficient (CTC) for reactions at the solid−liquid interface is shown to be linearly proportional to the electrochemical potential change from the initial state to the transition state as well the interface differential capacitance at the constant-charge model, and can be further related to the net dipole change normal to the surface during the reaction. Using the constant-charge theory, the CTC can be explicitly calculated on the basis of the first principles calculations without the need to assume the redox behavior of the elementary reactions and thus provide a unique possibility to evaluate and compare the magnitude of CTC for different reactions across different surfaces. By examining a series of interface reactions and comparing the calculated CTC values, we propose simple rules to understand and predict the charge transfer coefficient of three classes of the interface elementary reactions. The role of surface dipole, solvation, and molecular adsorption strength on the CTC can now be clarified from first principles calculations.

Charge Transfer Coefficient — First Principles Calculations

$$\beta = C_d \frac{\partial \Delta G}{\partial \sigma}$$

$$\alpha = \frac{S C_d \Delta \Phi}{\theta F}$$

$\alpha = 0.46$ $\alpha = -0.03$ $\alpha = -0.18$

1. INTRODUCTION

The electron transfer coupled with chemical bond making/breaking represents one of the most common reactions in physical world.[1,2] The rate of these reactions (electric current, i) could be enhanced dramatically by the external potential (U) as manifested by the Tafel equation (eq 1),[3−5] which states that overpotential (η) is proportional to the log i (a and b are constants, U_0 is the equilibrium potential), a unique property that has been greatly exploited to design a new synthetic route driven by electro-photo conditions. Although the model Hamiltonian approach has been utilized to treat the electron/ion transfer reactions,[6−10] the theoretical framework based on first principles calculations is still not available to compute the Tafel kinetics of the electron-coupled bond-making/-breaking processes at the solid−liquid interface. Here, we formulate a constant-charge representation for understanding and quantifying the kinetics of elementary reaction on surfaces, based on which the reactions at solid−liquid interface are classified in general and their activity−potential relations are predicted.

$$\eta = a + b \log i \quad (\eta = |U - U_0|) \tag{1}$$

$$b = -2.3RT/\alpha F \tag{2}$$

The traditional way to interpret the Tafel equation follows a 1-D potential energy surface (PES) crossing model similar to Marcus theory proposed for charge transfer reactions without chemical bond making/breaking. From this model, the Tafel slope b is derived to be reversely proportional to the so-called charge transfer coefficient (CTC) α in eq 2[11−15] (T is temperature and F is Faraday constant). The CTC α from Marcus definition denotes the coordinate of transition state (TS) in a conceived reaction coordinate for electron transfer, and thus is also called as symmetry factor. The CTC is often assumed to be ~0.5 for the single-electron transfer reaction by assuming a symmetrical PES crossing.

However, a great uncertainty arises for reaction on the solid/liquid interface, not least because the amount of electrons transferred in the elementary step cannot be assigned straightforwardly and the reactions catalyzed by surfaces often comprise a series of elementary steps.[16−19] In fact, the magnitude of the Tafel slope could vary from reaction to reaction and also depend on the catalysts, suggesting a complex nature of the CTC α. For example, the Tafel slope for methanol oxidation (a 4-electron oxidation to CO) on Pt ranges from 95 to 440 mV from different experimental groups,[20−22] and the Tafel slope of ~440 mV[22] measured by the recent experiment is particularly large ($\alpha = 0.14$; the rate increases with the increase of the potential). Similarly, for HCOOH oxidation on Pd/C, the Tafel slope is also large, 170 mV ($\alpha = 0.35$).[23] Consequently, the microscopic mechanism of

electrocatalytic reactions often cannot be resolved with merely the measured α.[24−28] The open question is how the CTC is influenced by the complex catalytic conditions at the atomic level, including the catalyst surface, solvent, and the type of chemical bond. It is thus highly desirable that the CTC of the electron-coupled bond-making/-breaking reactions can be computed accurately by modern electronic structure calculations, from which the fundmental understandings can be acheieved.

2. METHODOLOGY AND CALCULATION DETAILS

2.1. DFT Calculations. All DFT calculations were performed using the SIESTA package[29] with numerical atomic orbital basis sets[30] and Troullier−Martins norm conserving pesudopotentials.[31] The exchange-correlation functional utilized was at the generalized gradient approximation level, known as GGA-PBE.[32] The optimized double-ζ plus polarization basis set with extra diffuse function was employed for metals. The orbital-confining cutoff was determined from an energy shift of 0.010 eV. The energy cutoff for the real space grid used to represent the density was set as 150 Ry. The Quasi-Newton l-BFGS method was employed for geometry relaxation until the maximal forces on each relaxed atom were less than 0.05 eV/Å. To correct the zero-point energy (ZPE), the vibrational frequency calculations were performed via the finite-difference approach. Transition states (TSs) of the catalytic reaction were searched using our recently developed Constrained-Broyden-based TS-searching methods.[33,34]

To derive the free energy reaction profile, we first obtain the reaction energy of each step (strictly speaking, Helmholtz free energy change (ΔF) at 0 K, 0 bar) that is directly available from DFT total energy (ΔE) after the ZPE correction. For elementary surface reactions without involving the adsorption/desorption of gaseous or liquid molecules, ΔF at 0 K, 0 bar is a good approximation to the Gibbs free energy (ΔG) as the temperature T and pressure p contributions at the solid phase are small (vibrational entropy contribution ΔTS is generally below 0.05 eV at 300 K for an elementary surface reaction[35]). To compute the free energy change ΔG of elementary reactions involving gaseous or liquid molecules, such as oxygen, hydrogen, and water, the large entropy term at 298 K is essential to take into account. We utilize the standard thermodynamic data to obtain the temperature and pressure contributions for the G of the aqueous H_2O and gaseous H_2, which are −0.57 eV (the entropy contribution is −0.22 eV in solution) and −0.31 eV as compared to the total energy of the corresponding free molecule (E, 0 K), respectively.[36] The G of O_2 is derived as $G[O_2] = 4.92$ (eV) $+ 2G[H_2O] − 2G[H_2]$ by utilizing OER equilibrium at the standard conditions.

2.2. DFT-Based Modified Poisson−Boltzmann Approach for Electrochemistry. Our methodology for calculating electrocatalytic reactions has been described in recent publications.[37,38] Here, we briefly overview the framework of the current approach, focusing on how to calculate electrochemical potential and differential capacitance from periodic first principles calculations (more details are shown in the Supporting Information). The solid−liquid interface was described using the periodic continuum solvation model based on the modified Poisson−Boltzmann equation (CM-MPB), which can take into account the long-range electrostatic interaction due to the solvation of electrolyte.[37−39] The DFT/CM-MPB method has been utilized to calculate the electro-photo catalytic reactions at the solid−liquid inter-

faces,[40,41] and compute the fundamental properties of metal surfaces in solution, such as the potential of zero charge and the differential capacitance, where the calculated values show a good agreement with the available experimental data.[38]

It should be emphasized that all of the reactions in this work have been modeled using a long unit cell (>80 Å normal to the surface) with a large solvation region to properly describe the potential drop from the surface to the solution, in which the reaction occurs on both sides of the surfaces (a symmetrical slab). This is essential to measure accurately the electrochemical potential change for the reaction on going from IS to TS. For modeling reactions involving ions, both the implicit (CM-MPB) and the explicit (H_2O molecules) solvation need to be taken into account due to the strong polarization of the ionic species in solution. For example, for proton, H_3O^+, we must also include its first solvation shell to model the reacting proton in solution, that is, $H_3O^+(H_2O)_3$ in bulk solution and $H_3O^+(H_2O)_2$ at the solid−liquid interface (the rest of the solution is represented by the CM-MPB model). At the solid−liquid interface, two of its H's of H_3O^+ are hydrogen-bonded with the nearby water molecules, and the left H can interact with the surface electronegative species such as O_2, O, and OH. The explicit solvation has also been checked for other reactions by adding extra H_2O molecules near the reactants.

3. RESULTS AND DISCUSSION

To identify the fundamental rules governing the kinetics of the electron-coupled bond-making/-breaking process, here a theory based on a constant-charge reaction model is derived to compute CTC from quantum mechanics. We start by considering a generalized surface reaction, A → B, with the free energy change (from A to B) being ΔG, where A and B denote two different adsorbates, for example, the reactant and the product, respectively. We let the adsorbates A and B be at the same surface coverage θ with respect to exposed metal atoms (an assumption enforced in periodic slab calculations). A general barrier−potential expression at constant T, constant P, and constant n_i conditions from fundamental thermodynamics can be established from Taylor expansion, and the first-order approximation is as in eq 3.

$$\Delta G = \Delta G_0(U_0) - \alpha F(U - U_0) = \Delta G_0(U_0) - \beta(U - U_0) \tag{3}$$

In eq 3, $\Delta G_0(U_0)$ is the free energy difference of the two states at the equilibrium potential U_0, and the coefficient β is the first derivative of the energy difference with respect to the potential, as shown in eq 4, which can be regarded as the constant-potential representation of coefficient β ($\Delta G(U)$ is a function of potential).

$$\beta = \frac{\partial \Delta G}{\partial U} \tag{4}$$

It should be noted that eq 3 does not assume the number of electrons transferred in the A → B conversion because the exact number of electrons transferred in an elementary reaction on surface is often poorly defined due to the delocalization of Fermi electrons of electrode. It is the purpose of this work that by deriving the equations, we can determine the number of electrons transferred explicitly for any A → B reaction on the surface from first principles calculations, instead of guessing from chemical intuition.

For eq 4, we can equally rewrite the derivative with respect to the surface free charge (i.e., net charge) and obtain eq 5 by

relating to differential capacitance C_d, that is, $\partial\sigma/\partial U$, and σ is the surface charge density (free charge per area). For chemical reactions on surfaces, the differential capacitance C_d should be a constant during a reaction from A to B. This is because the reaction on the surface is a rare event; that is, when one particular reaction occurs, the composition of the whole surface can be considered the same and so does the C_d at the interface. From our calculations based on DFT/CM-MPB, we can systematically enlarge the unit cell employed for investigating the reactions to examine whether the C_d is varied during the reaction. We found that by using the large enough unit cell, typically around $p(4 \times 4)$ (16 atoms per layer) as utilized here, the effect to the C_d due to the structural change of reactants is largely diminished and the C_d remains quite constant (see Supporting Information S-Table 1 for the reactions investigated in this work).

$$\beta = \frac{\partial\sigma}{\partial U}\left(\frac{\partial G_B}{\partial\sigma} - \frac{\partial G_A}{\partial\sigma}\right)$$

$$\beta = C_d\frac{\partial\Delta G_{A\to B}}{\partial\sigma} \tag{5}$$

By changing the derivative from eq 4 to eq 5, we now need to compute $\Delta G(\sigma)$ instead of $\Delta G(U)$. Both the $\partial G/\sigma$ and C_d terms are quantities that can be obtained from first principles calculations, as discussed below. It should be mentioned that the C_d value can be measured from experiment and thus serves as a benchmark for theoretical calculations.[38,42]

To compute C_d and $\partial G/\partial\sigma$ from first principles, we utilize the numerical approach based on the located intermediate states (i.e., IS, TS, and FS) at each surface charge condition (see the Supporting Information). Within the first principles DFT framework, the surface charge can be tuned by adding/extracting total charges in the system. We have utilized our recently developed periodic continuum solvation model following the modified Poisson–Boltzmann equation (DFT/CM-MPB),[37,38,41] to compute these values, in which the neutralizing charge of the system is distributed in the continuum solution region following the MPB equation. The symmetric slab must be utilized with reactions occurring on both sides of the slab. This is essential to analyze accurately the response of the reaction quantities, including the total energy and the absolute electrode potential, to the change of charges. In Figure 1, we show the typical plot for the potential U and G of a surface system with respect to σ, in which the derivative can be readily obtained by linear fitting.
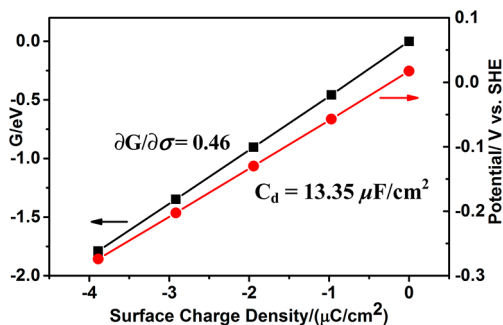

Figure 1. The plot of the potential (U) and the free energy (G) of a 1 ML H covered Pt(111) surface with respect to the surface charge density σ based on DFT/CM-MPB calculations.

Equation 5 can be further simplified to eq 6 by using the general DFT theorem, $\partial G/\partial\sigma = \Phi$, where Φ is the absolute electrode potential and S is the unit surface area (e.g., the area of one surface Pt atom on Pt surface).

$$\beta = \frac{SC_d\Delta\Phi}{\theta} \tag{6}$$

$$\alpha = \frac{C_d}{F}\frac{\partial\Delta G_{A\to B}}{\partial\sigma} = \frac{SC_d\Delta\Phi}{\theta F} \tag{7}$$

Apart from eq 5, eq 6 can also be utilized directly for computing the coefficient β. Instead of computing $\partial G/\partial\sigma$ using the linear plot as shown in Figure 1, we can measure the relative potential change ($\Delta\Phi$) from the A to the B state, which is in fact even simpler in computation. The only concern is the accuracy of $\Delta\Phi$ in first principles calculations, which is often a more sensitive quantity to compute compared to the total energy change (ΔG). By extensive DFT/CM-MPB calculations with carefully converged $\Delta\Phi$ (e.g., via symmetrical surface calculations and long unit cell with a large solvation region for screening), as shown below, we demonstrate that the ΔG and $\Delta\Phi$ expressions in eq 7 do yield consistent results (see Table 1).

Table 1. Numerical Results for Calculating CTC of 12 Reactions on the Surface

reaction[a]	$\Delta\Phi_0$ (V)[b]	Θ (ML)[b]	C_d ($\mu F/cm^2$)[c]	α[d]	α[e]
1	0.67	1/12	13.47	0.46	0.46
2	0.60	1/16	13.44	0.50	0.55
3	0.43	1/16	16.82	0.49	0.49
4	−0.04	1/12	13.35	−0.03	−0.03
5	0.15	1/6	15.87	0.10	0.06
6	−0.08	1/6	15.21	−0.04	−0.03
7	−0.05	1/16	17.66	−0.04	−0.06
8	−0.02	1/16	17.38	−0.06	−0.03
9	0.08	1/16	13.53	0.02	0.07
10	0.01	1/16	21.87	−0.04	0.01
11	0.19	1/16	18.07	0.22	0.24
12	−0.16	1/16	18.07	−0.18	−0.20

[a]All of the reactions are on the Pt(111) surface. (1) H + H_3O^+(aq) + e → H_2 + H_2O, (2) O_2 + H_3O^+(aq) + e → O + OH + H_2O, (3) O + H_3O^+(aq) + e → OH + H_2O, (4) H + H→ H_2, (5) CO + O → CO_2, (6) CO + OH→ COOH, (7) CH_2OH + H → CH_3OH, (8) CH_3O + H → CH_3OH, (9) O_2 → O + O, (10) $CH_3CH_2OH–(H_2O)_2$ → $CH_3CHOH–(H_2O)_2$ + H, (11) $CH_3OH–2(H_2O)_2$ → $CH_3O–2(H_2O)_2$ + H, (12) $CH_3OH–(H_2O)_2$ → $CH_2OH–(H_2O)_2$ + H. The reaction conditions modeled (including the electrochemical potential, the coadsorbed species with the reactants) for these reactions are described in Supporting Information S-Figure 1. [b]$\Delta\Phi_0$ refers to the change of the absolute electrode potential from IS to TS at the zero surface charge condition, and θ is the coverage of the reactant (with respect to exposed metal atoms), as utilized in eqs 6 and 7. [c]C_d is the differential capacitance. [d]α is calculated using the ΔG expression in eq 7. [e]α is calculated using the $\Delta\Phi$ expression in eq 7.

On the basis of the transition state theory, we can let the A and B states be the IS and TS of an elementary surface reaction, respectively, and arrive at the general expression for CTC at the constant charge representation by relating α with β. Therefore, the CTC α can be calculated using eq 7, via either ΔG (eq 5) or $\Delta\Phi$ (eq 6). It is noticed that by the definition in eq 3, the CTC can be negative, reflecting the trend for the barrier decrease induced by the elevation of potential and vice versa. As

compared to the traditional constant-potential representation, the constant-charge representation provides a straightforward, computable formula to assess the CTC of the reaction on surface without assuming the number of electrons transferred during a reaction. The factors influencing the CTC are wrapped into the change of the absolute electrode potential during the reaction.

It should also be emphasized that the constant-charge method proposed here is to calculate the CTC of an elementary reaction step. However, the transfer coefficient obtained from the Tafel slope in experiment is in fact the apparent (effective) transfer coefficient, which may not correspond to one particular elementary reaction step. The computation of the overall CTC of the multiple reaction process can be done once the reaction profile is known and the rate-determining step is resolved by kinetics modeling, as shown in our previous work for H_2O oxidation, oxygen reduction, and hydrogen evolution reactions.[28,37,39] Indeed, only after the CTC of the elementary steps are computed and understood, can the overall CTC of the multiple reaction process be derived and compared to the experimental apparent CTC.

In this work, we have determined the Tafel relationship of 12 typical elementary reactions on surface using the constant charge representation theory, including hydrogen evolution, oxygen evolution, methanol oxidation, ethanol oxidation, and CO oxidation on the Pt(111) surface. Their reaction formula may be formally written as (1) $H + H_3O^+(aq) + e \rightarrow H_2 + H_2O$, (2) $O_2 + H_3O^+(aq) + e \rightarrow O + OH + H_2O$, (3) $O + H_3O^+(aq) + e \rightarrow OH + H_2O$, (4) $H + H \rightarrow H_2$, (5) $CO + O \rightarrow CO_2$, (6) $CO + OH \rightarrow COOH$, (7) $CH_2OH + H \rightarrow CH_3OH$, (8) $CH_3O + H \rightarrow CH_3OH$, (9) $O_2 \rightarrow O + O$, (10) $CH_3CH_2OH-(H_2O)_2 \rightarrow CH_3CHOH-(H_2O)_2 + H$, (11) $CH_3OH-2(H_2O)_2 \rightarrow CH_3O-2(H_2O)_2 + H$, (12) $CH_3OH-(H_2O)_2 \rightarrow CH_2OH-(H_2O)_2 + H$. Except for the solvated proton (H_3O^+) that is present explicitly in water solution (above surface), as indicated by aq in parentheses, all other species involved in these reaction can be considered as adsorbed species on the surface in contact with the solution environment. The number of electrons transferred in these elementary reactions is not known a priori except that for reactions involving solvated protons (H_3O^+), one electron transfer is assumed. These reactions include the common C−H, O−H, C−O, H−H chemical bond making and breaking. The solvation of these reactions at the interface was described by including both the first solvation shell with explicit water molecules, if necessary (for treating the short-range strong polarization), and the implicit solvation via CM-MPB (for treating the long-range solvent−molecule interaction). The data for calculating CTC using eq 7 are shown in Table 1, and more details on how to calculate these values from first principles are given in the Supporting Information.

All of the computed CTC of the reactions have been plotted in Figure 2, against the geometrical reaction coordinate of the TS, x^{TS}. x^{TS} is a 1-D geometrical measure of the position of the TS by projecting the TS structure onto the x-axis (reaction coordinate) defined by the IS (at $x = 0$) and the FS (at $x = 1$). All of the optimized structures of these reactions, including the ISs and TSs, are shown in Supporting Information S-Figure 1.

From Figure 2, we can see that these elementary reactions can be broadly divided into three classes. For Class I, the barrier ΔG_a is strongly dependent on U with a large α, being around ±0.5. There are three reactions in this class, $H + H_3O^+$, $O_2 +$
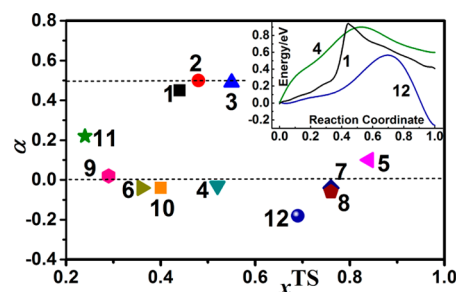

Figure 2. The plot for the computed CTC of the reactions against the reaction coordinate of the TS, x^{TS}. The reaction coordinates of the IS and the FS are defined as zero and one in x-axis, respectively. These reactions can be broadly classified into three classes: Class I contains (1) $H + H_3O^+(aq) + e \rightarrow H_2 + H_2O$, (2) $O_2 + H_3O^+(aq) + e \rightarrow O + OH + H_2O$, (3) $O + H_3O^+(aq) + e \rightarrow OH + H_2O$. Class II contains (4) $H + H \rightarrow H_2$, (5) $CO + O \rightarrow CO_2$, (6) $CO + OH \rightarrow COOH$, (7) $CH_2OH + H \rightarrow CH_3OH$, (8) $CH_3O + H \rightarrow CH_3OH$, (9) $O_2 \rightarrow O + O$, (10) $CH_3CH_2OH-(H_2O)_2 \rightarrow CH_3CHOH-(H_2O)_2 + H$. Class III contains (11) $CH_3OH-2(H_2O)_2 \rightarrow CH_3O-2(H_2O)_2 + H$, (12) $CH_3OH-(H_2O)_2 \rightarrow CH_2OH-(H_2O)_2 + H$. The inset illustrates the reaction profile of selected reactions in three classes (1, 4, 12). Also see the Supporting Information for the optimized structures of the reactions.

H_3O^+, $O + H_3O^+$ reaction, and their CTC values are calculated to be 0.46, 0.50, and 0.49, respectively. All of these reactions involve the participation of a solution H_3O moiety to react with a surface adsorbate, and the reaction can generally be written as $A + H_3O^+ + e \rightarrow BH + H_2O$ with one electron transfer. Shown in Figure 3 are the reaction snapshots of such an electron-coupled proton transfer reaction ($H + H_3O^+$).

The calculated α value being ~0.5 in Class I agrees with the general assumption in electrochemistry.[43] We found that the geometrical position of the TS (x_{TS}) is also close to 0.5, indicating the TS locates symmetrically between the IS and the
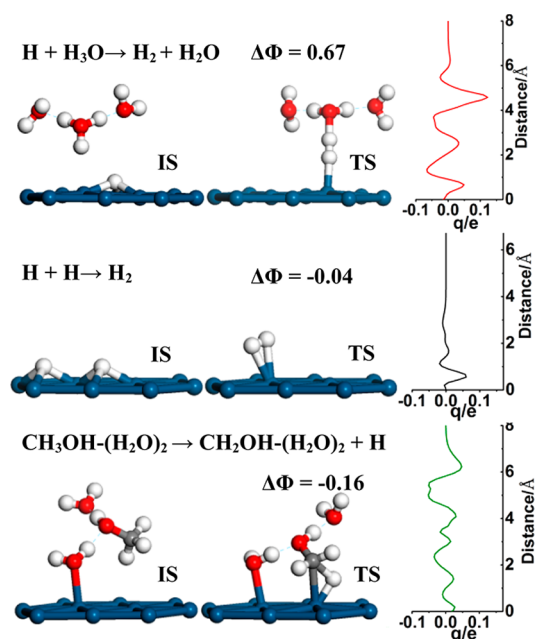

Figure 3. The reaction snapshots (IS and TS) of typical reactions in three classes. The change of the net charge from IS to TS along the surface normal direction is also shown to indicate the change of the dipole layer.

FS. Obviously, these reactions follow the Eley–Rideal mechanism as their counterpart at the solid–gas interface, where a coming reactant outside the surface reacts with the surface species.

For Class II, the barrier ΔG_a is weakly dependent on U with the coefficient α diminishing to zero. Belonging to this class are most of the reactions at the solid–liquid interface investigated with a clear Langmuir–Hinswood mechanism, where two adsorbed species combine to form a new product or one molecule dissociates into two fragments, that is, A + B ↔ AB. For example, the α for the H + H → H_2 is essentially zero (−0.03). No matter what kind of chemical bond (e.g., H–H, O–O, C–H, O–H, C–O) is involved, we found that the barriers of these reaction, associative or dissociative, are generally insensitive to the potential, indicating essentially no surface dipole change in the reaction.

Class III contains the exception cases, in which the value of α is unconventional, being neither close to ±0.5 nor to zero. Shown in Figure 2, we identify two reactions at the solid–liquid interface both related to CH_3OH dissociation, the initial O–H bond breaking with the α of 0.22 and the initial C–H bond breaking with the α of −0.18. The large α indicates that these two reactions could formally be written as $CH_3OH-(H_2O)_2$ → $CH_3O-(H_2O)_2^{q-}$ + H + q^+, and $CH_3OH-(H_2O)_2$ → $CH_2OH-(H_2O)_2^{q+}$ + H + q^-, which is consistent with the polarization character of the CH_3O and CH_2OH fragments.

It should be mentioned that the classification of reactions according to CTC has been suggested previously in electrochemistry.[44−48] By using the model Hamiltonian approach, the CTC of the bond-breaking reaction was investigated by Schmickler's group,[6,49−51] and they pointed out that the CTC value may deviate from the Marcus value of 0.5 for both the simple electron transfer reaction and the reaction with electron transfer and bond breaking due to the symmetry breaking. The metal d-band, solvent, and bond coordinate may all influence the value of CTC, but the quantification of the role of these key elements still requires a number of parameters in the model Hamiltoninan. With first principles calculations in combination with the CM-MPB method, here we show that the CTC value can now be calculated, which allows the role of the electrode surface, the solvent, and the bond type to be rationalized at the atomic level.

Now we are at the position to discuss the significance of the current theoretical model. To better understand the variation of CTC from reaction to reaction, we can further relate the potential change ($\Delta\Phi$) in eq 7 to the change of surface dipole layer ΔP_z, because only the surface dipole along the surface normal z direction matters for the work function. In such a way, we can obtain eq 8, where ε_0 is the vacuum permittivity, ε_r is the relative permittivity of the surface dipole layer, Q is a distribution of the net charge at the interface, and the integral of the surface dipole runs over the reaction complex space Ω (whole slab in periodic calculations).

$$\alpha = \frac{C_d}{F}\left(\frac{P_z}{\varepsilon_r\varepsilon_0}\right)_A - \frac{C_d}{F}\left(\frac{P_z}{\varepsilon_r\varepsilon_0}\right)_B = \frac{C_d}{F\varepsilon_r\varepsilon_0}\Delta P_z$$

$$= \frac{C_d}{F\varepsilon_r\varepsilon_0}\Delta\left(\int_\Omega Qd_z\, d\Omega\right) \tag{8}$$

It is noted that eq 8 has one approximation in that the surface dipole layer containing adsorbed A and B has the same value of ε_r. From the Gouy–Chapman–Stern theory of

electrical double layer,[3] the constant term $C_d/\varepsilon_r\varepsilon_0$ can in fact be approximated to be the reverse of the height (x_H) of the compact Helmholtz layer, $x_H = \varepsilon_r\varepsilon_0/C_d$, which is a value of 3−4 Å for most adsorbates on surfaces. Obviously, eq 8 indicates that the CTC will not be zero as long as the surface dipole differs on going from IS to TS, which could be influenced by a number of factors, including the charge transfer during the reaction, the solvation, and the surface polarization induced by reaction. Below, we utilize eq 8 to understand the trend of CTC in the three classes of electrocatalytic reactions.

First, eq 8 can be utilized to predict the CTC because the surface dipole change of a reaction can be estimated largely according to the IS structure. In general, for the reaction with one electron/proton passing through the compact Helmholtz layer, the change of the surface dipole can be estimated to be close to the height of the compact layer. Considering that $C_d/\varepsilon_r\varepsilon_0$ approximately equals the reverse of the height of the compact layer, it is reasonable that the charge transfer coefficient is close to 1 for the one-electron transfer reaction. For such reactions, the TS locates between the IS and FS, and the apparent charge transfer coefficient is thus close to 0.5. On the other hand, when two adsorbates react with each other, the surface dipole should not be significantly changed from the IS to the TS, and thus CTC is close to zero considering that the TS of reaction on metal surfaces generally mimics the IS due to the strong adsorption strength of the common adsorbates (being unsaturated fragments).[52] These can be seen clearly from the change of the net charge from IS to TS for H + H_3O^+ + e → H_2 + H_2O and H + H → H_2, shown in Figure 3, where the charge redistribution in the former reaction is much more pronounced, which extends to 4 Å above the surface.

Second, the solvent may influence the magnitude of CTC markedly and lead to unconventional CTC values. This could occur when the solvation shell reforms during the reaction at the solid/liquid interface. For the reactions investigated, we found that the methanol dissociation in Class III experiences a remarkable change in the solvation shell. We have shown in Figure 3 the IS and TS of the C–H bond breaking of methanol dissociation. As shown, at the IS the methanol is not in direct contact with the surface but hydrogen-bonded with adsorbed H_2O; at the TS methanol moves to the surface to break its C–H bond. Consequently, the change of the net charge from IS to TS is also obvious in the reaction, which oscillates even at a height 6 Å above the surface (Figure 3). Interestingly, our calculated CTC (0.18) is close to the recent experimental measurement in methanol oxidation (0.14),[22] suggesting that the initial C–H bonding (reaction 12) is the rate-determining step of methanol oxidation and the solvation plays critical role in the kinetics. A comprehensive comparison between theory and experiment for methanol oxidation (containing many elementary steps) is beyond the scope of this work and will be discussed in the future publication. The unconventional CTC of CH_3OH dissociation could thus be attributed to the strong polarization of the newly emerged fragments at the TS (CH_3O- and $-CH_2OH$) surrounded by water solution. The first principles calculation results provide the theoretical evidence that the CTC is sensitive to the bond polarization as well as the solvation.

4. CONCLUSION

To recap, this work develops a constant-charge reaction theory for computing the potential-dependent kinetics of elementary reactions at the solid–liquid interface. The CTC for reactions

E

at the solid−liquid interface is shown to be linearly proportional to the electrochemical potential change from the IS to the TS as well as the interface differential capacitance at the constant-charge model, and can be further related to the net dipole change normal to the surface during the reaction.

On the basis of the constant charge theory, extensive first-principles calculations were performed to evaluate the CTC of a series of reactions at the Pt/H_2O interface involving the common O−O, C−H, O−H, H−H bond breaking/formation. We found that these reactions can be classified into three types, and the origin of the CTC is thus discussed in terms of the surface dipole and solvation. In short, the three classes can be described as follows: (i) The first is the Eley−Rideal type where one reactant comes into solution to react with the adsorbate on the surface. The CTC of this type of elementary reaction is around 0.5. (ii) The second type is the Langmuir−Hinshelwood type where reactants adsorb on the surface to recombine or dissociate. The CTC of this type of elementary reaction is around zero. (iii) The third is the exceptional case where the CTC is neither zero nor close to 0.5. The reactions belong to this class could involve the dramatic change of the solvation shell from IS to TS and thus induce a large surface dipole change during the reaction. We expect the theoretical methods and model utilized here to evaluate the CTC of elementary reaction based on first principles calculations can be applied in general for understanding processes at the solid−liquid interface, in particular to clarify the catalytic role of the surface dipole, solvation, and molecular adsorption strength on the potential-dependent kinetics.

■ ASSOCIATED CONTENT

Ⓢ Supporting Information

Detail of our methodology for investigating electrocatalysis, the reaction condition modeled for the 12 reactions and the reaction snapshots from DFT/CM-MPB calculations, the calculation details and located ISs and TSs of the reactions, and the calculated C_d of the 12 reactions on the surface at TS and IS. This material is available free of charge via the Internet at http://pubs.acs.org.

■ AUTHOR INFORMATION

Corresponding Author

*E-mail: zpliu@fudan.edu.cn.

Notes

The authors declare no competing financial interest.

■ ACKNOWLEDGMENTS

■ REFERENCES

(1) Bonnet, N.; Marzari, N. First-Principles Prediction of the Equilibrium Shape of Nanoparticles under Realistic Electrochemical Conditions. *Phys. Rev. Lett.* **2013**, *110*, 086104.

(2) Karlberg, G. S.; Jaramillo, T. F.; Skulason, E.; Rossmeisl, J.; Bligaard, T.; Norskov, J. K. Cyclic Voltammograms for H on Pt(111) and Pt(100) from First Principles. *Phys. Rev. Lett.* **2007**, *99*, 126101.

(3) Bard, A. J.; Faulkner, L. R. *Electrochemical Methods: Fundamentals and Applications*, 2nd ed.; John Wiley & Sons Inc.: New York, 2001.

(4) Chen, W. F.; Sasaki, K.; Ma, C.; Frenkel, A. I.; Marinkovic, N.; Muckerman, J. T.; Zhu, Y.; Adzic, R. R. Hydrogen-Evolution Catalysts Based on Non-Noble Metal Nickel-Molybdenum Nitride Nanosheets. *Angew. Chem., Int. Ed.* **2012**, *51*, 6131−6135.

(5) Cao, B.; Veith, G. M.; Diaz, R. E.; Liu, J.; Stach, E. A.; Adzic, R. R.; Khalifah, P. G. Cobalt Molybdenum Oxynitrides: Synthesis, Structural Characterization, and Catalytic Activity for the Oxygen Reduction Reaction. *Angew. Chem.* **2013**, *125*, 10953−10957.

(6) Schmickler, W. Recent Progress in Theoretical Electrochemistry. *Annu. Rep. Prog. Chem., Sect. C: Phys. Chem.* **1999**, *95*, 117−162.

(7) Ignaczak, A.; Schmickler, W. Effects of Friction and Asymmetric Inner Sphere Reorganization Energy on the Electron Transfer Reaction Rate—Two-Dimensional Simulations. *Electrochim. Acta* **2007**, *52*, 5621−5633.

(8) Grimminger, J.; Schmickler, W. Dynamics of Combined Electron and Proton Transfer at Metal Electrodes. *Chem. Phys.* **2007**, *334*, 8−17.

(9) Schmickler, W. Electronic Effects in the Electric Double Layer. *Chem. Rev.* **1996**, *96*, 3177−3200.

(10) Mohr, J.-H.; Schmickler, W. Exactly Solvable Quantum Model for Electrochemical Electron-Transfer Reactions. *Phys. Rev. Lett.* **2000**, *84*, 1051.

(11) Petrii, O. A.; Nazmutdinov, R. R.; Bronshtein, M. D.; Tsirlina, G. A. Life of the Tafel equation: Current understanding and Prospects for the Second Century. *Electrochim. Acta* **2007**, *52*, 3493−3504.

(12) Streeter, I.; Compton, R. G. Mass Transport Corrected Tafel Analysis of Voltammetric Waves: When can It be Applied? *Electrochim. Acta* **2007**, *52*, 4305−4311.

(13) Albu, T. V.; Anderson, A. B. Studies of Model Dependence in an Ab Initio Approach to Uncatalyzed Oxygen Reduction and the Calculation of Transfer Coefficients. *Electrochim. Acta* **2001**, *46*, 3001−3013.

(14) Skulason, E.; Tripkovie, V.; Bjorketun, M. E.; Gudmundsdottir, S.; Karlberg, G.; Rossmeisl, J.; Bligaard, T.; Jonsson, H.; Norskov, J. K. Modeling the Electrochemical Hydrogen Oxidation and Evolution Reactions on the Basis of Density Functional Theory Calculations. *J. Phys. Chem. C* **2010**, *114*, 18182−18197.

(15) Kanan, M. W.; Nocera, D. G. In Situ Formation of an Oxygen-Evolving Catalyst in Neutral Water Containing Phosphate and Co^{2+}. *Science* **2008**, *321*, 1072−1075.

(16) Wang, J. X.; Markovic, N. M.; Adzic, R. R. Kinetic Analysis of Oxygen Reduction on Pt(111) in Acid Solutions: Intrinsic Kinetic Parameters and Anion Adsorption Effects. *J. Phys. Chem. B* **2004**, *108*, 4127−4133.

(17) Jaramillo, T. F.; Jørgensen, K. P.; Bonde, J.; Nielsen, J. H.; Horch, S.; Chorkendorff, I. Identification of Active Edge sites for Electrochemical H_2 Evolution from MoS_2 Nanocatalysts. *Science* **2007**, *317*, 100−102.

(18) Surendranath, Y.; Kanan, M. W.; Nocera, D. G. Mechanistic Studies of the Oxygen Evolution Reaction by a Cobalt-Phosphate Catalyst at Neutral pH. *J. Am. Chem. Soc.* **2010**, *132*, 16501−16509.

(19) Björketun, M. E.; Tripkovic, V.; Skúlason, E.; Rossmeisl, J. Modeling of the Symmetry Factor of Electrochemical Proton Discharge via the Volmer Reaction. *Catal. Today* **2013**, *202*, 168−174.

(20) Housmans, T.; Koper, M. Methanol Oxidation on Stepped Pt [n (111)×(110)] Electrodes: a Chronoamperometric Study. *J. Phys. Chem. B* **2003**, *107*, 8557−8567.

(21) Lu, G.-Q.; Chrzanowski, W.; Wieckowski, A. Catalytic Methanol Decomposition Pathways on a Platinum Electrode. *J. Phys. Chem. B* **2000**, *104*, 5566−5572.

(22) Liu, S. X.; Liao, L. W.; Tao, Q.; Chen, Y. X.; Ye, S. The Kinetics of CO Pathway in Methanol Oxidation at Pt Electrodes, a Quantitative Study by ATR-FTIR Spectroscopy. *Phys. Chem. Chem. Phys.* **2011**, *13*, 9725−9735.

(23) Liu, Y.; Wang, L. W.; Wang, G.; Deng, C.; Wu, B.; Gao, Y. High Active Carbon Supported PdAu Catalyst for Formic Acid Electro-

F

dx.doi.org/10.1021/jp411531f | *J. Phys. Chem. C* XXXX, XXX, XXX−XXX

oxidation and Study of the Kinetics. *J. Phys. Chem. C* **2010**, *114*, 21417−21422.

(24) Wu, G.; More, K. L.; Johnston, C. M.; Zelenay, P. High-Performance Electrocatalysts for Oxygen Reduction Derived from Polyaniline, Iron, and Cobalt. *Science* **2011**, *332*, 443−447.

(25) Liang, Y.; Li, Y.; Wang, H.; Zhou, J.; Wang, J.; Regier, T.; Dai, H. Co3O4 Nanocrystals on Graphene as a Synergistic Catalyst for Oxygen Reduction Reaction. *Nat. Mater.* **2011**, *10*, 780−786.

(26) Markovic, N. M.; Grgur, B. N.; Ross, P. N. Temperature-Dependent Hydrogen Electrochemistry on Platinum Low-index Single-Crystal Surfaces in Acid Solutions. *J. Phys. Chem. B* **1997**, *101*, 5405−5413.

(27) Greeley, J.; Stephens, I. E. L.; Bondarenko, A. S.; Johansson, T. P.; Hansen, H. A.; Jaramillo, T. F.; Rossmeisl, J.; Chorkendorff, I.; Norskov, J. K. Alloys of Platinum and Early Transition Metals as Oxygen Reduction Electrocatalysts. *Nat. Chem.* **2009**, *1*, 552−556.

(28) Wei, G.-F.; Fang, Y.-H.; Liu, Z.-P. First Principles Tafel Kinetics for Resolving Key Parameters in Optimizing Oxygen Electrocatalytic Reduction Catalyst. *J. Phys. Chem. C* **2012**, *116*, 12696−12705.

(29) Soler, J. M.; Artacho, E.; Gale, J. D.; Garcia, A.; Junquera, J.; Ordejon, P.; Sanchez-Portal, D. The SIESTA Method for Ab Initio Order-N Materials Simulation. *J. Phys.: Condens. Matter* **2002**, *14*, 2745−2779.

(30) Junquera, J.; Paz, O.; Sanchez-Portal, D.; Artacho, E. Numerical Atomic Orbitals for Linear-Scaling Calculations. *Phys. Rev. B* **2001**, *64*, 235111.

(31) Troullier, N.; Martins, J. L. Efficient Pseudopotentials for Plane-Wave Calculations. *Phys. Rev. B* **1991**, *43*, 1993−2006.

(32) Perdew, J. P.; Burke, K.; Ernzerhof, M. Generalized Gradient Approximation Made Simple. *Phys. Rev. Lett.* **1996**, *77*, 3865−3868.

(33) Wang, H. F.; Liu, Z. P. Comprehensive Mechanism and Structure-Sensitivity of Ethanol Oxidation on Platinum: New Transition-State Searching Method for Resolving the Complex Reaction Network. *J. Am. Chem. Soc.* **2008**, *130*, 10996−11004.

(34) Shang, C.; Liu, Z.-P. Constrained Broyden Minimization Combined with the Dimer Method for Locating Transition State of Complex Reactions. *J. Chem. Theory Comput.* **2010**, *6*, 1136−1144.

(35) Hong, Q.-J.; Liu, Z.-P. Mechanism of CO_2 Hydrogenation over Cu/ZrO$_2$ (2□12) Interface from First-Principles Kinetics Monte Carlo Simulations. *Surf. Sci.* **2010**, *604*, 1869−1876.

(36) Lide, R. D. *CRC Handbook of Chemistry and Physics*, 84th ed.; CRC Press: New York, −2004.

(37) Fang, Y. H.; Liu, Z. P. Mechanism and Tafel Lines of Electro-Oxidation of Water to Oxygen on RuO(2)(110). *J. Am. Chem. Soc.* **2010**, *132*, 18214−18222.

(38) Fang, Y. H.; Wei, G. F.; Liu, Z. P. Theoretical Modeling of Electrode/Electrolyte Interface from First-Principles Periodic Continuum Solvation Method. *Catal. Today* **2013**, *202*, 98.

(39) Fang, Y.-H.; Wei, G.-F.; Liu, Z.-P. Catalytic Role of Minority Species and Minority Sites for Electrochemical Hydrogen Evolution on Metals: Surface Charging, Coverage, and Tafel Kinetics. *J. Phys. Chem. C* **2013**, *117*, 7669−7680.

(40) Shang, C.; Liu, Z.-P. Origin and Activity of Gold Nanoparticles as Aerobic Oxidation Catalysts in Aqueous Solution. *J. Am. Chem. Soc.* **2011**, *133*, 9938−9947.

(41) Li, Y.-F.; Liu, Z.-P.; Liu, L.; Gao, W. Mechanism and Activity of Photocatalytic Oxygen Evolution on Titania Anatase in Aqueous Surroundings. *J. Am. Chem. Soc.* **2010**, *132*, 13008−13015.

(42) Cuesta, A. Measurement of the Surface Charge Density of CO-saturated Pt(111) Electrodes as a Function of Potential: the Potential of Zero Charge of Pt(111). *Surf. Sci.* **2004**, *572*, 11−22.

(43) Damjanov, A.; Dey, A.; Bockris, J. O. M. Kinetics of Oxygen Evolution and Disslution on Platinum Electrodes. *Electrochim. Acta* **1966**, *11*, 791−814.

(44) Schmickler, W. Electron and Ion Transfer Reactions on Metal Electrodes. *Electrochim. Acta* **1996**, *41*, 2329−2338.

(45) Kuznetsov, A.; Schmickler, W. A Simulation of an Electro-chemical Adiabatic Electron-Transfer Reaction. *Chem. Phys. Lett.* **2000**, *327*, 314−318.

(46) Schmickler, W.; Mohr, J. The Rate of Electrochemical Electron-Transfer Reactions. *J. Chem. Phys.* **2002**, *117*, 2867.

(47) Kuznetsov, A.; Nazmutdinov, R.; Schmickler, W. Monte Carlo Simulation of Electrochemical Electron Transfer Processes. *J. Electroanal. Chem.* **2002**, *532*, 171−180.

(48) Conway, B. Electrochemical Oxide Film Formation at Noble Metals as a Surface-Chemical Process. *Prog. Surf. Sci.* **1995**, *49*, 331−452.

(49) Santos, E.; Schmickler, W. Fundamental Aspects of Electro-catalysis. *Chem. Phys.* **2007**, *332*, 39−47.

(50) Schmickler, W. A Theory for Nonadiabatic Electrochemical Electron-Transfer Reactions Involving the Breaking of a Bond. *Chem. Phys. Lett.* **2000**, *317*, 458−463.

(51) Ignaczak, A.; Schmickler, W. Simulations of Adiabatic Bond-Breaking Electron Transfer Reactions on Metal Electrodes. *Chem. Phys.* **2002**, *278*, 147−158.

(52) Liu, Z.-P.; Hu, P. General Trends in CO Dissociation on Transition Metal Surfaces. *J. Chem. Phys.* **2001**, *114*, 8244−8247.